Measurement: Sensors 20-21 (2022) 100368

Contents lists available at ScienceDirect

Measurement: Sensors

journal homepage: www.sciencedirect.com/journal/measurement-sensors

Highly sensitive fluorescence-based mercury(II) DNA sensor enhanced by silver(I) activation

Noorhayati Idros [a,*], Katherine Stott [b], Jasmina Allen [c], Varun S. Kamboj [a], Warren T. Corns [c], Peter J. Newton [a], Hernán Verde-Luján [d], Luis De Los Santos Valladares [a,e,f], Carlos Villanueva [g], Jorge H. Jhoncon [h,i], Daping Chu [j], Crispin.H.W. Barnes [a]

[a] Department of Physics, Cavendish Laboratory, University of Cambridge, 19 JJ Thomson Avenue, Cambridge, CB3 0HE, United Kingdom
[b] Department of Biochemistry, University of Cambridge, Sanger Building, 80 Tennis Court Road, Cambridge, CB2 1GA, United Kingdom
[c] P S ANALYTICAL, Arthur House, Crayfields Industrial Estate, Main Road, Orpington, Kent, BR5 3HP, United Kingdom
[d] Universidad Nacional de Barranca, Avenida Toribio de Luzuriaga N° 376, M J, Urbanización La Florida, Barranca, Lima, Republic of Peru
[e] School of Materials Science and Engineering, Northeastern University, No 11, Lane 3, Wenhua Road, Heping District, Shenyang, 110819, People's Republic of China
[f] Laboratorio de Ceramicos y Nanomateriales, Facultad de Ciencias Fısicas, Universidad Nacional Mayor de San Marcos, Ap. Postal 14–0149, Lima, 15081, Republic of Peru
[g] Universidad Nacional de Cañete, Jr. San Agustin 124, San Vicente de Cañete Lima, Republic of Peru
[h] Centro de Investigación en Agricultura Orgánica. Facultad de Ciencias, Universidad Nacional de Educación Enrique Guzmán y Valle, Av. Enrique Guzmán y Valle s/n Lima, 15472, Lima, Republic of Peru
[i] Centro Internacional de Investigación para la Sustentabilidad (CIIS). Universidad Nacional de Cañete, Jr. San Agustín N° 124 San Vicente de Cañete, 15701, Cañete, Republic of Peru
[j] Department of Engineering, Centre for Advanced Photonics & Electronics, University of Cambridge, 9 JJ Thomson Avenue, Cambridge, CB3 0FA, United Kingdom

ARTICLE INFO

Keywords:
Metal-DNA complexes
Structure-switching DNA
Mercury(II) detection
Silver(I) activator
Fluorescence sensor

ABSTRACT

Mercury exposure constitutes an acute risk to human health and the environment. Driven by the requirement to monitor trace-level mercury, we report a highly sensitive mercury(II) DNA sensor enhanced by silver(I) activation, followed by mercury(II)-specific oligonucleotides (MSO) molecular configuration switch and mercury(II)-modulated FRET. Activating the MSO strands with silver(I), mismatched cytosine–silver(I)–cytosine bridges induce individual MSO strands to fold readily in response to mercury(II) resulting in enhanced fluorescence signal. The structural switches were studied by 2D ^{1}H–^{1}H NOESY and TOCSY NMR spectroscopy, and 260 nm absorbance. The signal decreases with increasing mercury(II) concentration from 100 pM to 0.1 mM. The approach affords outstanding mercury(II) selectivity over other environmentally associated metals. Furthermore, the methodology was deployed for detection of mercury(II) in spiked pond waters with 97.9–100.6% recovery. The simple and feasible format has great potential for developing a cost effective and useful tool for environmental monitoring.

1. Introduction

Mercury, one of the highly toxic environmental metal contaminants, originates from a range of natural and anthropogenic sources, for instance, solid waste incineration, gold production, and the combustion of fossil fuels [1–3]. Even at low levels, mercury exposure poses a risk to human health and the environment, throwing bodily mechanisms into disarray, resulting in brain damage, kidney failure, and the destruction of the cardiovascular system [4–6]. One of the stable and prevalent forms of mercury contamination is the water-soluble divalent mercuric ion (Hg^{2+}) [7], which is extensively distributed in water, soil, and the atmosphere. Hg^{2+} infiltrates the body and accumulates [8–10]. The U.S. Environmental Protection Agency (EPA) and World Health Organization (WHO) have stringently defined the safe limits of Hg^{2+} concentration in drinkable water to be lower than 2 μg/L (10 nM) (EPA, U.S., 2001) [11]. Therefore, it is very important to be able to measure and analyse Hg^{2+} present in an environment such as water rapidly, sensitively, and selectively. Monitoring of Hg^{2+} levels in water, particularly, is paramount with regard to environmental analysis, toxicology, water safety, water quality, and waste management [12]. Currently the conventional

* Corresponding author.
E-mail address: ni245@cam.ac.uk (N. Idros).

https://doi.org/10.1016/j.measen.2022.100368
Received 29 November 2021; Received in revised form 21 February 2022; Accepted 11 March 2022
Available online 19 March 2022

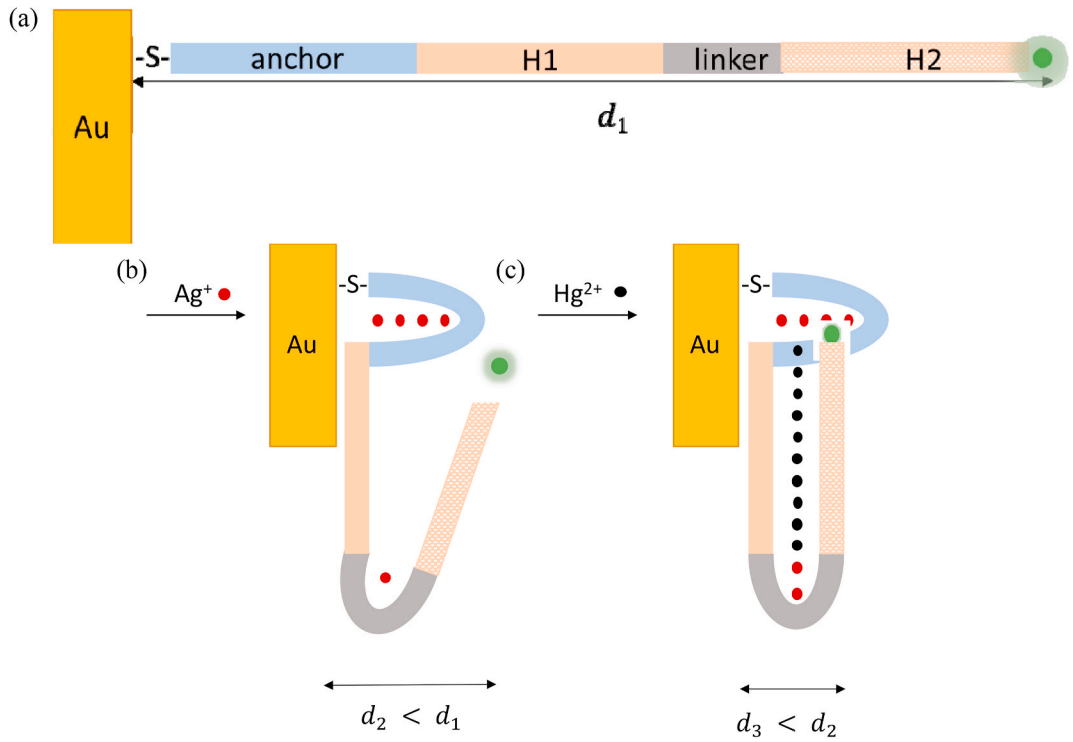

Scheme 1. The proposed two-step sensing mechanism. (a) The CT-DNA probe consists of anchor and linker fragments that are consecutive cytosine mismatches while H1 and H2 are Hg^{2+}-binding sequences rich in thymine mismatches; the probe is covalently linked to an Au surface; (b) C–Ag^{+}-C bridges are activated by cooperative Ag^{+} binding in step 1; and (c) Hg^{2+} stabilizes a hairpin-like structure by forming T-Hg^{2+}-T bridges. d_1, d_2 and d_3 are the lengths between FAM and Au in the case of original CT-DNA, Ag^{+} activation, and Hg^{2+} binding, respectively.

detection methods for Hg^{2+} ions primarily consist of cold atomic fluorescence [13], cold atomic absorption spectrophotometry [14], inductively coupled plasma mass spectrometry (ICP-MS) [15–17] atomic fluorescence spectroscopy (AFS) [18] and atomic absorption spectroscopy (AAS) [19,20]. However, these techniques involve complicated procedures or costly instruments, which makes them inconvenient, complicated, time-consuming and unsuitable for portable use.

To address these problems, several types of sensing platforms have been developed using organic fluorophores [21,22], chromophores [23–25], proteins [26], anodic stripping voltammetry [27,28], and polymeric materials [29]. Most of these sensors, however, are limited due to poor selectivity with severe interference from other metal ions, low sensitivity (current limit of detection >100 nM), and incompatibility with aqueous environments. More promising strategies for Hg^{2+} measurement utilise oligonucleotides as a recognition molecule and are rapid, low-cost, and suitable for real-time detection [30,31]. DNA is an exceptionally effective, bio-specific and eco-friendly analytical reagent for the determination of heavy metal ions [32]. It was reported that Hg^{2+} ions can bind specifically in between two DNA thymine bases, promoting these T–T mismatches to form stable base pairs [33, 34]. T–Hg^{2+}–T oligonucleotide base-pairing has high specificity due to the selective coordination of Hg^{2+} to T bases, with a binding constant even higher than a T-A Watson-Crick pair (Tanaka et al., 2007) [34,35]. Various DNA-based methods of detection of Hg^{2+} have been developed, such as colorimetry [36–41], electrochemistry [42–44], Raman spectroscopy/scattering [45–51], field effect transistors [52,53], and surface plasmon resonance [54,55] amongst others. In addition, many researchers have carried out Hg^{2+} detection using methods based on fluorescence resonance energy transfer (FRET) [56–59].

Among the various detection techniques, fluorescence changes are the most convenient due to the simplicity of the detection format and low detection limit [60–63]. Ono and Togashi [33] developed the first fluorescence Hg^{2+} biosensor with a mercury-specific oligonucleotide (MSO). The MSO probe comprised a fluorophore and a quencher at its 5′ and 3′ termini, respectively. In the absence of Hg^{2+}, the MSO existed as a random coil, and the fluorophore was isolated from the quencher, generating a large fluorescence signal. In the presence of Hg^{2+}, the probe formed a hairpin structure and pulled the fluorophore and the quencher close enough for the FRET effect [64,65]. This "turn-off" sensor was reported to have a limit of detection (LOD) of 40 nM. Based on the DNA conformational switch [66] and FRET strategy, great flexibility, and multifunction for Hg^{2+} was achieved by simply modifying the sequences of the probes. For example, Chang et al. [67] reported a fluorescent thrombin-binding aptamer (TBA) probe (5′-GGTTGGTGTGGTTGG-3′) for selective detection of Hg^{2+} and Pb^{2+} ions with different masking reagents; changes in fluorescence intensity allowed the selective detection of Hg^{2+} and Pb^{2+} ions at 5 nM and 300 pM in the presence of a random DNA/NaCN mixture and phytic acid, respectively. Wang et al. [68] designed a multifunctional DNA probe for the simultaneous detection of Hg^{2+} and silver(I), Ag^{+}. They constructed an OR logic gate by taking Hg^{2+} and Ag^{+} as input and changes in fluorescence intensity as output. With this probe, the reported limit of Hg^{2+} detection is 35 pM, which is more sensitive than other methods.

While mercury binding to thymine bases is a widely exploited concept, further innovations are needed to increase the sensitivity of mercury detection. In this study, we report a use of silver(I) or Ag^{+} ions as a mercury sensor activator, which extends the limits of mercury sensing to a new level. The probe consists of separate silver- and mercury-activated regions, functionalized onto gold (Au) surfaces through Au–thiol covalent bonds. Detection is through a two-step sensing mechanism with activation of cytosine-Ag^{+}-cytosine mismatch bridges prior to mercury detection. Silver(I) activation induces folding of single-stranded DNA (known as 'CT-DNA') into double strand as observed from absorbance of UV light at 260 nm.

In the first sensing step, C–Ag^{+}-C bridges on the short linker and longer anchor fragment (Scheme (a) are formed by Ag^{+} binding, which is likely to be cooperative for the longer anchor fragment but is also effective for the shorter linker fragment as shown by NMR spectroscopy.

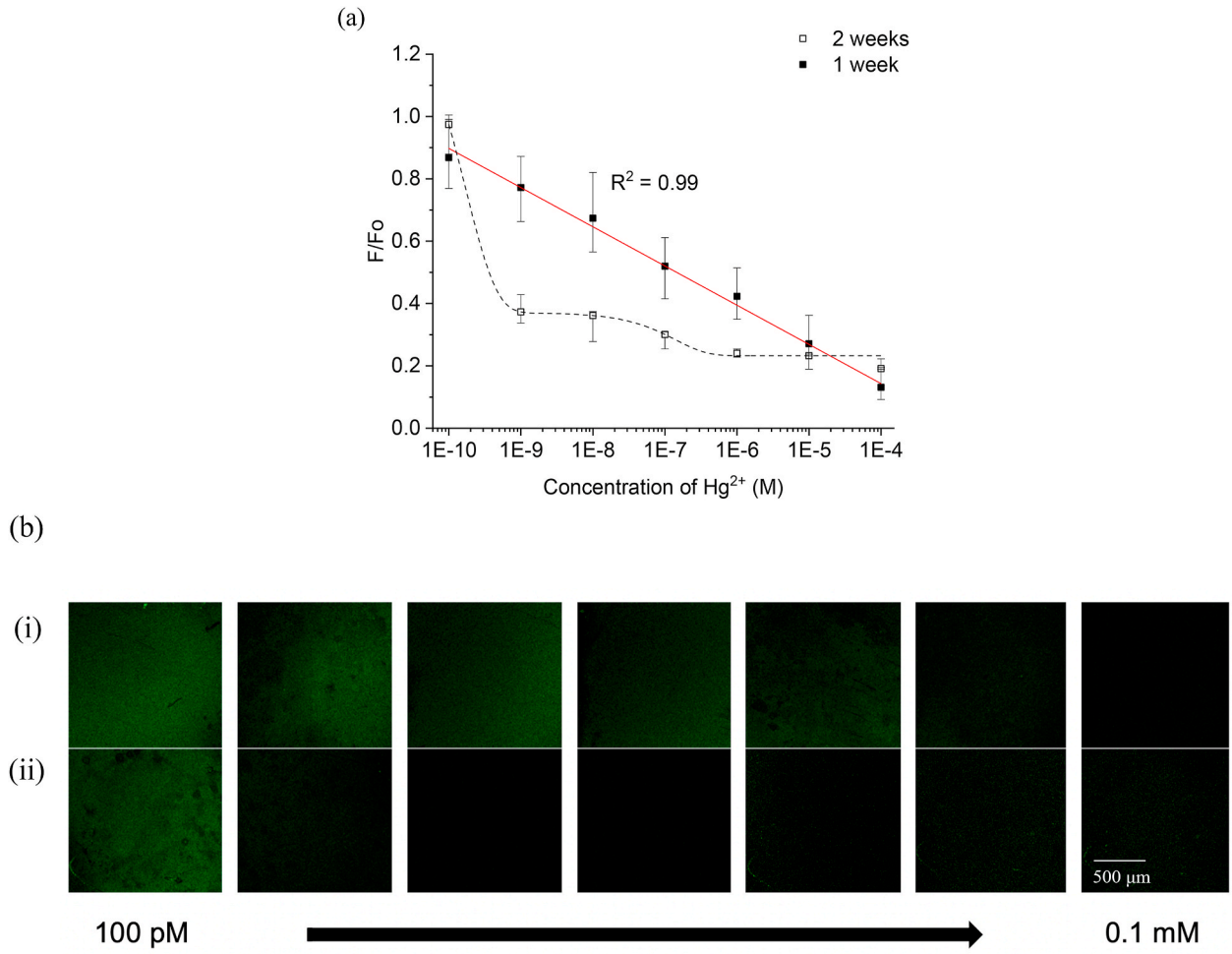

Fig. 1. (a) Relative fluorescence intensity (F/F_o) and (b) corresponding fluorescence images of Au-CT-DNA-FAM vs Hg^{2+} concentration. F_o is the Au-CT-DNA-FAM intensity prior to addition of Hg^{2+}, and F is the intensity of Au-CT-DNA-FAM following incubation with Hg^{2+}, measured at 1 (b (i)) and 2 (b (ii)) weeks following preparation. The fluorescence signal in (b) is pseudo-colored using the confocal microscope look-up table.

By introducing Hg^{2+} in the second step, mercury further stabilizes the incipient hairpin-like structure by forming Hg^{2+}-induced T-Hg^{2+}-T bridges between the H1 and H2 fragments.

As a result, the distance between FAM and Au (d) decreased dramatically (Scheme 1 (c); ($d_3 < d_2$ (Ag^+ stabilization) $< d_1$ (original length of CT-DNA)), which enables an enhanced FRET process between the energy donor (FAM) and the energy acceptor (Au). Thus, the fluorescence of FAM is efficiently quenched in the presence of Hg^{2+} ions. The structural change generates a fluorescence signal that is highly sensitive and specific to Hg^{2+}, so the fluorescence intensity of Au-CT-DNA-FAM probes will decrease with the addition of Hg^{2+} ions only. It is known that the Hg–N_3 bond in T-Hg^{2+}-T is more ionic than covalent in character [69]. This ionic nature enables Hg^{2+} to act as an electron acceptor, which can quench fluorescence through electron transfer from the labelled fluorophore to the T-Hg^{2+}-T pair [70].

Combining Ag^+ activation and with T–Hg^{2+}–T folding of the probe in the presence of Hg^{2+} significantly reduces the error range of the fluorescence signal with a dynamic range from 100 pM to 0.1 mM. The LOD is more than one order of magnitude lower than that reported when using some of the most sensitive probes to date: DNAzymes, and other reported MSO-based Hg^{2+} sensors. It is also two-orders of magnitude lower than the Hg^{2+} safe limit of 2 µg/L (10 nM) reported by the U.S. Environmental Protection Agency [11]. Our approach affords outstanding Hg^{2+} selectivity over other environmentally associated metal ions. Furthermore, the methodology was deployed for detection of Hg^{2+} in spiked pond waters with 97.9–100.6% recovery.

2. Materials and methods

Single-stranded DNA was purchased from Integrated DNA Tec hnologies. The 37-mer probe has a sequence of 5′—SH-CCC CCCCCCCTCTTCTTTCTTCCCCCTTGTTTGTTGT-FAM; modified with a thiol group (—SH) and fluorescein (FAM) on its 5′ and 3′ ends, respectively. The sequence is referred to as 'CT-DNA' herein, due to its high C- and T-content and is divided into parts: anchor (CCCCCCCCCC) and linker (CCCCC), which are cytosine-rich Ag^+ binding sites, and thymine-rich Hg^{2+} binding sequences H1 (TCTTCTTTCTT) and H2 (TTGTTTGTTGT). The stock DNA probe was first resuspended in 10 mM Tris-HCl pH 7.4, 1 mM EDTA, and stored at –20 °C overnight. For each assay, 99 µL of 0.2 µM DNA probe was used. For NMR measurements, an unmodified oligo with the same 37-mer sequence was used, plus a further unmodified 27-mer oligo based on the 37-mer sequence minus the anchor (TCTTCTTTCTTCCCCCTTGTTTGTTGT). Oligos were suspended in 10 mM sodium phosphate pH 6.0. Gold (Au) surfaces were cleaned with Piranha solution (30% hydrogen peroxide (H_2O_2) and 98% sulphuric acid (H_2SO_4)). Tris(2-carboxyethyl)phosphine hydrochloride (TCEP), 6-mercapto-1-hexanol (MCH), hydrochloric acid (HCl), and metal salts such as mercury(II) nitrate monohydrate, silver(I) nitrate, arsenic(III) chloride, lead(II) chloride, copper(II) chloride, and iron(III) chloride were purchased from Sigma Aldrich. The metal salts were prepared in 18 MΩ/cm ultrapure water (ddH_2O). 1 mM TCEP and MCH were also prepared in ddH_2O. 1 mM of TCEP was prepared fresh each time before use. Tris-acetate (TA) buffer, 0.2 M, pH 7.4 was purchased

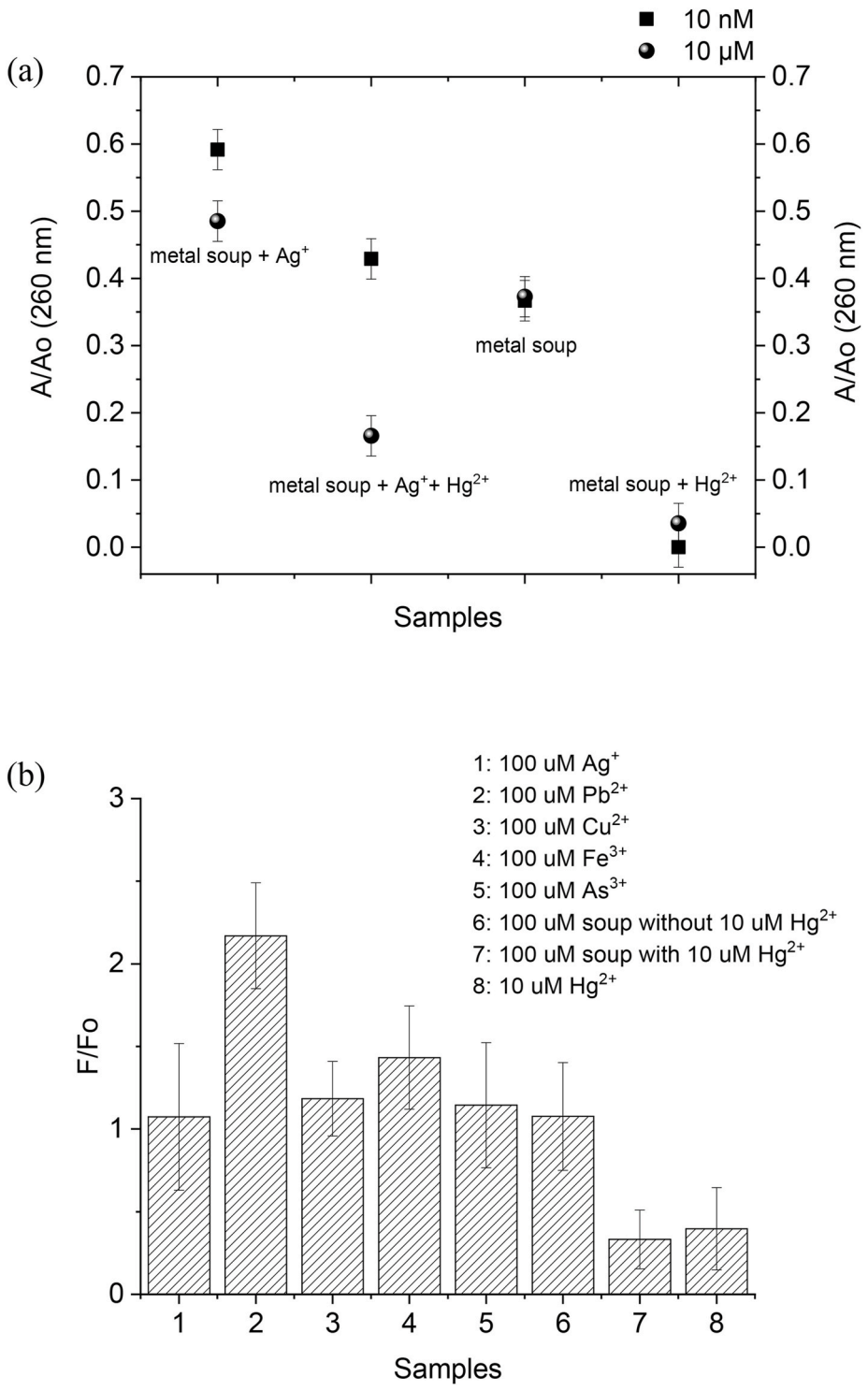

Fig. 2. Selectivity of the sensor: (a) A_{260} relative to the baseline (A/A_o); A_o is the Au-CT-DNA-FAM intensity and A is the intensity of Au-CT-DNA-FAM-metals. Metal soup contains a mixture of Cu^{2+}, As^{3+}, Fe^{3+} and Pb^{2+}, and was tested with and without added Ag^{+} and Hg^{2+}, (b) selectivity to Hg^{2+} under the influence of environmentally relevant metal ions.

from Generon. 25 mM TA, pH 7.4 (storage buffer) and 50 mM TA, pH 7.4 (reaction buffer) were prepared in ddH_2O from stock. Functionalization of the CT-DNA probe on Au surfaces was performed in 10 mM Tris-HCl pH 7.4, 1 mM EDTA, 0.1 M NaCl, 10 mM TCEP (attach buffer).

2.1. Surface preparation of Au

Silicon wafers were cut into 0.5 cm × 0.5 cm samples and cleaned by immersion in acetone and isopropanol. Samples were then loaded into a thermal evaporator, which was pumped to a base pressure of $3x10^{-7}$ mbar. A 20 nm titanium film was deposited first as an adhesion layer, followed by a 200 nm Au film. The Au surface was cleaned with a mixture of 1 part 30% H_2O_2 to 4 parts of 98% concentrated H_2SO_4 at room temperature for 5 min. After that, the cleaned Au substrates were rinsed with ddH_2O and then dried under a stream of nitrogen (N_2) gas.

2.2. Surface functionalization of CT-DNA on Au

1 μL of 1 mM TCEP was added to 99 μL of 0.2 μM CT-DNA probe and incubated for 2 h at room temperature. Subsequently, an equal volume of the TCEP-activated CT-DNA probe and attach buffer (solution 1) were mixed in a vial. For each assay, 60 μL of solution 1 was used to functionalize the CT-DNA probe on the Au surface by incubation for 18 h in a humidity chamber at room temperature. Following this, the sample was rinsed with copious ddH_2O and dried with a N_2 gun. The functionalized sample was then passivated using 100 μL of 1 mM MCH solution in a humidity chamber for 2 h at room temperature, rinsed several times with ddH_2O, and dried with a N_2 gun. The functionalized sensor (Au-CT-DNA-FAM) was stored in storage buffer at 4 °C prior to fluorescence measurement. Parts of the protocols were based on published methods [71–73].

2.3. Two-step sensing

In the first step, aliquots (100 μL) of reaction buffer (50 mM TA, pH 7.4) containing 100 pM Ag^+ were incubated with Au-CT-DNA-FAM at room temperature for 15 min. In the second step, 50 μL of various Hg^{2+} concentrations were added and incubated for an additional 15 min. Fluorescence spectra relative to baseline (F/F_o) were measured on a Leica SP5 Inverted Confocal at room temperature, in a dark room; where F_o and F are the intensities of Au-CT-DNA-FAM and Au-CT-DNA-FAM-Hg^{2+}, respectively. The fluorescence from microscopy images was determined in ImageJ [74] by extracting the average fluorescence values from 50 × 50 pixels at six-ten different areas.

3. Results and discussion

3.1. Sensitivity and stability

The linearity and sensitivity of the sensor were tested using Hg^{2+} concentrations spanning a wide range (100 pM - 0.1 mM), and the stability of the sensor was assessed by repetition of the measurements after two weeks of storage (Fig. 1). The response curve (Fig. 1(a)) demonstrates that the relative fluorescence signal (F/F_o) decreases in response to increasing concentrations of Hg^{2+}. The response measured within the first week of sensor preparation (solid squares) is linear and exhibits a broad dynamic range from 100 pM to 0.1 mM. However, after two weeks, the signal decreased significantly (open squares) and the corresponding fluorescence images in Fig. 1 (b) indicate a significant reduction of the signal of more than 50% in the presence of 1 nM and greater Hg^{2+}. The sensor is, thus, stable for application within one week after preparation.

3.2. Selectivity

Au-CT-DNA-FAM specificity was examined through absorbance at 260 nm (A_{260}; Fig. 2 (a)), since a reduction would likely indicate folding of the CT-DNA probe on binding Hg^{2+}. Purine and pyrimidine bases in DNA absorb ultraviolet light at 260 nm strongly. Double-stranded DNA absorbs ~25% less UV light than single-stranded DNA at room temperature [75] due to the formation of hydrogen bonds and stacking of bases, termed 'hypochromicity' [76]. Hg^{2+}-induced folding was tested in a background of environmentally relevant metal ions (Ag^+, Cu^{2+}, As^{3+}, Fe^{3+} and Pb^{2+}). The effect of adding Ag^+ was tested separately, since the C-rich regions of the sensor are predicted to bind Ag^+. To test the sensitivity of the system, the assay was also performed under two very different Hg^{2+} concentrations (10 nM and 10 μM). All added metals induced hypochromicity, with the samples containing 10 μM Hg^{2+} displaying the strongest effect. However, the presence of Ag^+ resulted in a strong concentration-dependent response to added Hg^{2+} (compare 'metal soup + Ag^+ + Hg^{2+},' with 'metal soup + Hg^{2+}'). Given the evidence for strong chelation of Ag^+ by C-rich DNA regions [77], formation of C–Ag^+–C bridges appears to increase differentiation in response to Hg^{2+} concentrations. The Au-CT-DNA-FAM thus has good sensitivity and selectivity for sensing Hg^{2+} in samples where Ag^+ is present.

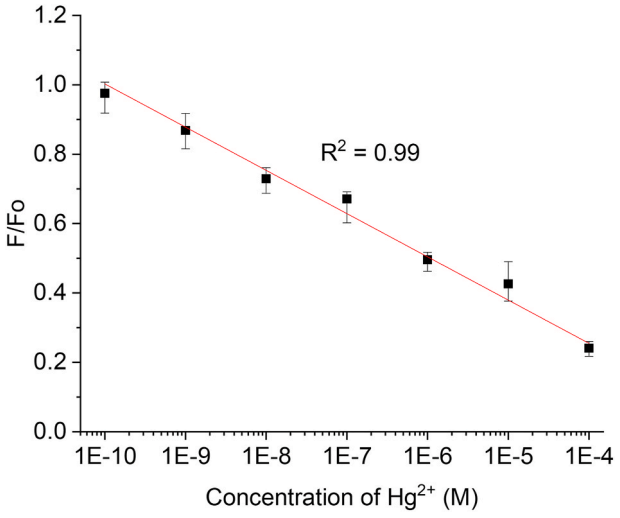

Fig. 3. Linear calibration curve of the response to Hg^{2+} after the probe following addition of Ag^+. Results of regression analysis: F/F_o = (–0.126 ± 0.004) log [Hg^{2+}] + (–0.360 ± 0.024) over the range 100 pM - 0.1 mM (R^2 = 0.99).

The fluorescence intensity of the system was tested and found to be both sensitive and selective to Hg^{2+} but not sensitive to other ions (Fig. 2 (b)). It is important to prevent false positives in the environmental water samples where various interfering ions or unspecific quenchers may exist. Thus, the Hg^{2+} appears to be both quantitatively and selectively determined through the fluorescence quenching of the Au-CT-DNA-FAM coupled with Ag^+ stabilization.

Regression analysis was performed to calibrate the response of the sensor to Hg^{2+} with Ag^+ present (Fig. 3). The response demonstrated good linearity (R^2 = 0.99) over a concentration range of 100 pM to 0.1 mM and was found to follow: F/F_o = (–0.126 ± 0.004) log [Hg^{2+}] + (–0.360 ± 0.024). The proposed method yields a limit of detection for Hg^{2+} ions of 100 pM with a much-reduced error range than the one demonstrated in Fig. 1 (a). Thus, this approach offers a sensitivity towards Hg^{2+} ions that is more than one order of magnitude lower than that reported for some of the most sensitive probes to date based on DNAzymes [78–80] and other reported "turn-off" MSO-based Hg^{2+} sensors [81,82]. The LOD of the sensor is also two-orders of magnitude lower than the Hg^{2+} safe limit reported by the U.S. EPA.

3.3. Metallo-DNA folding

The mechanism of coupled binding and folding of DNA in the presence of Hg^{2+} and Ag^+ was studied by ^{1}H NMR spectroscopy, using 2D ^{1}H–^{1}H NOESY and TOCSY NMR experiments. The design of the CT-DNA probe (^{1}CCCCCCCCCCTCTTCTTTCTTCCCCCTTGTTTGTTGT^{37}) provides two potential Cyt-rich, Ag^+-condensable regions, termed 'anchor' (^{1}CCCCCCCCCC^{10}) and 'linker' (^{22}CCCCC^{26}). While both regions were expected to bind Ag^+, we first wished to establish whether Ag^+ binding to the central linker region was indeed promoting hairpin formation, as intended by the design. Therefore, for simplicity, experiments were first performed on a 27-mer anchor-deleted construct (^{11}TCTTCTTTCTTCCCCCTTGTTTGTTGT^{37}) and repeated in the presence of Ag^+(aq). Free metal ions were removed at the end of the titration by exchange of the buffer. The free oligo (Fig. 4(a)) showed poor chemical-shift dispersion of the three guanine (G) and eight cytosine (C) residues, presumably due to the lack of any folding and the similarity of their chemical environment: 3 C are flanked by other C (as CCC), and all three G are flanked by thymine (T) (as TGT). In contrast, the 16 T

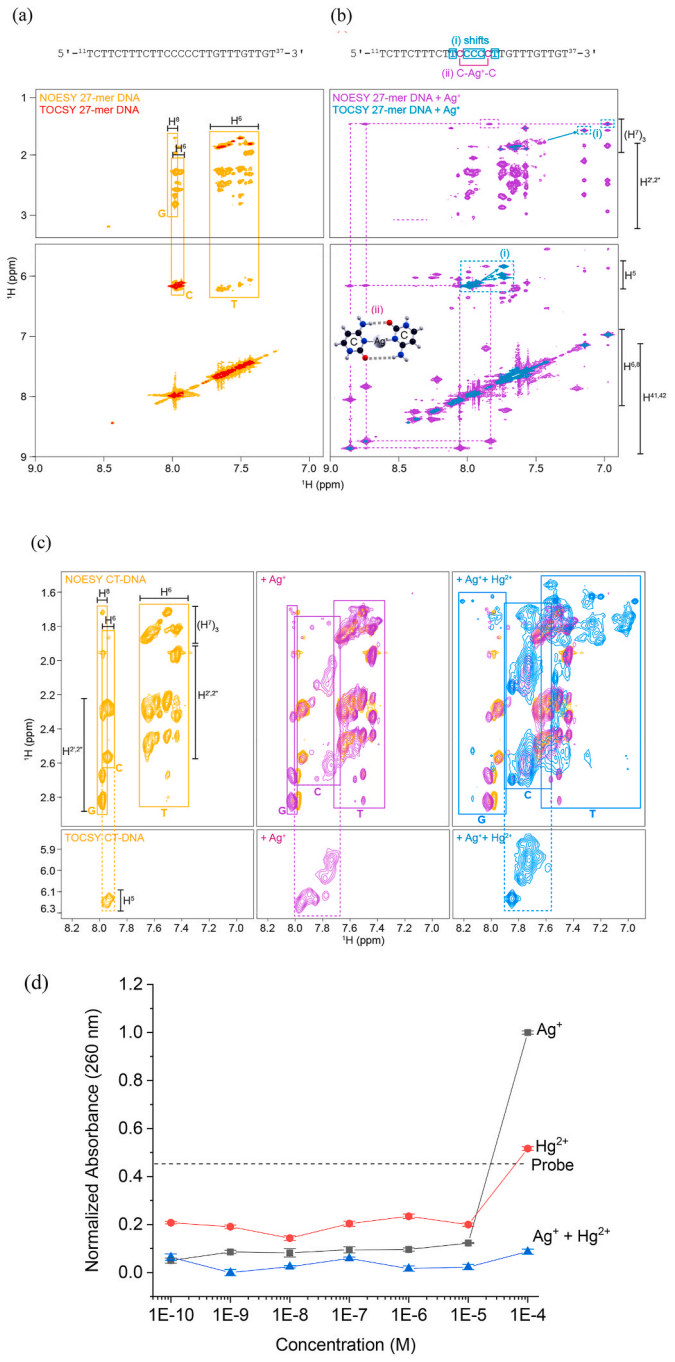

Fig. 4. Study of metallo-DNA folding and surface topology by means of (a–c) NMR and (d) UV absorbance. (a) 2D ^{1}H–^{1}H NOESY and TOCSY NMR experiments of 27-mer anchor-deleted CT-DNA alone (yellow and red, respectively), and (b) in the presence of 5 × Ag^{+} (purple and turquoise, respectively). Turquoise boxed regions in (b) indicate TOCSY cross-peaks of C H^5–H^6 and T $(H^7)_3$–H^6 that shift. Purple dotted lines show NOE connectivity to newly detectable C NH_2 resonances (H^{41} and H^{42}) indicative of C–Ag^{+}-C. (c) NOESY and TOCSY of full length 37-mer CT-DNA (yellow) showing the changes to the spectra on sequential addition of Ag^{+} (purple) and Hg^{2+} (blue) to a molar excess of 10 × CT-DNA. The aromatic/aliphatic correlation regions of the NOESY spectra reveal the chemical-shift dispersion of the three residue types (boxed). C H^6 residues were assigned by comparison with TOCSY spectra that exclusively reveal C H^5–H^6 cross-peaks in the aromatic/aromatic correlation region (dotted boxes). (d) Normalized A_{260} of CT-DNA (probe), Ag^{+}, Hg^{2+} and (Ag^{+} + Hg^{2+}). (For interpretation of the references to color in this figure legend, the reader is referred to the Web version of this article.)

residues showed intrinsically greater chemical-shift dispersion, presumably due to their variable sequence context (4 × CTT, 3 × TTC, 2 × TTT, 3 × TTG, 2 × GTT and one GT at the 3' terminus). Assignment of the central strip of C residues in the aromatic region was clear from the TOCSY experiments, in which the C H^5–H^6 cross-peaks (that are unique in this region) served as a guide, and G and T residues were easily distinguished by their characteristic H^8 and H^6 chemical shifts, respectively. On addition of Ag^{+} (Fig 4(b)), two major changes were seen: (i) three cytosine H^5–H^6 and two thymine H^6-$(H^7)_3$ TOCSY cross-peaks underwent a large shift, and (ii) several new peaks appeared in the NOESY from newly detectable pairs of Cyt NH_2 resonances (H^{41} and H^{42}). (These peaks were absent in the spectrum of metal-free DNA, which is expected for exposed amino protons that exchange freely with the solvent.) Furthermore, two NH_2 pairs (shown by purple dotted lines in Fig. 4(b)) were connected by several mutual NOEs. These were attributed to formation of a new Ag^{+}-bridged ^{22}C–Ag^{+}-C^{26} base pair, which would be expected to yield two new inter-base hydrogen bonds within the NOE-detectable distance range of each other, consistent with hairpin formation. The large shifts seen for the three H^5–H^6 TOCSY cross-peaks (shown by turquoise dotted lines in Fig. 4(b)) are consistent with a large conformational change incurred to the central ^{23}CCC^{21} of the hairpin. The two upfield-shifted Thy H^6 resonances (also shown by turquoise dotted lines) could be assigned sequence-specifically to the Thy residues flanking the linker (^{21}TCCCCCT^{27}), *via* mutual NOE connectivity between the methyl groups and the two new pairs of Cyt NH_2 resonances.

The experiments were repeated using the full length 37-mer CT-DNA, and with Ag^{+}(aq) and Hg^{2+}(aq), added sequentially (Fig. 4 (c)). As for the 27-mer, the NMR spectra of the free 37-mer CT-DNA were consistent with an extended single-stranded oligonucleotide. The central strip of C residues in the aromatic region was distinguished by H^5–H^6 cross-peaks in the TOCSY, and G and T by their characteristic H^8 and H^6 chemical shifts, respectively. On addition of Ag^{+} ions, some peaks from the C region were observed to shift upfield and broaden out to different extents. These observations are consistent with the formation of C–Ag^{+}-C complexes and the selectivity of Ag^{+} for C residues, as observed previously (Ono et al., 2008) [77]. The peak broadening is consistent with chemical exchange between energetically-similar conformations (since the Ag^{+} is now presumably dynamically partitioned between the anchor and linker) and/or a loss of conformational freedom on folding. On addition of Hg^{2+} ions, the most dramatic changes were seen to the G and T resonances, which shifted and broadened considerably, consistent with the formation of T-Hg^{2+}-T bridges [33–35], and their direct proximity to G residues. These observations are consistent with a global conformational folding event that would be expected to occur following pairing of T residues. Smaller shifts and some peak broadening were also seen for C residues. The shift of the C resonances away from their original positions in the metal-free oligo was only complete following addition of both metal ions, implying that C–Ag^{+}-C complexes were further stabilized by formation of the T-Hg^{2+}-T complexes. No evidence was seen of direct C-G base pairing in the imino region of the spectrum (not shown), but this does not exclude the possibility that dynamic pairing occurs.

Fig. 4 (d) depicts the A_{260} by the CT-DNA probe in the presence of Ag^{+}, Hg^{2+} and both Hg^{2+} and Ag^{+} (Ag^{+} + Hg^{2+}). Silver (I) induces folding of single-stranded CT-DNA strand into double strand as observed from absorbance of UV light at 260 nm. Combining Ag^{+} and folding of the probe in the presence of Hg^{2+} significantly reduces the error range of the fluorescence signal with a dynamic range from 100 pM to 0.1 mM. This observation is consistent with stacking interactions between cytosine bases with silver, and thymine bases with mercury, and indicates a higher degree of folding of the CT-DNA probe in the presence of both metals.

Table 1
Detection of Hg^{2+}concentrations in environment water samples by the proposed method and CV-AFS (P. M. is proposed method). Data are given as Mean ± SD.

Water samples	Spiked $[Hg^{2+}]$/ pM	P. M. $[Hg^{2+}]$/ pM	P. M. Recovery (%)	AFS $[Hg^{2+}]$/ pM	AFS Recovery (%)
Deionized Water	149.6	146.6 ± 11.6	97.9	128.7 ± 8.1	86.0
Payne's pond	149.6	149.7 ± 19.0	100.1	141.7 ± 9.2	94.8
West Café pond	149.6	150.4 ± 7.7	100.6	162.1 ± 12.0	108.4

3.4. Applicability

The sensitivity and selectivity of the method to Hg^{2+} was tested using actual environmental water samples. A standard Hg^{2+} solution of 149.6 pM (30 ppt) was added to samples of water from three sources: deionized water, Payne's pond and West Café pond, in triplicate. The linear equation $F/F_o = (–0.126 \pm 0.004) \log [Hg^{2+}] + (–0.360 \pm 0.024)$ was used to estimate the corresponding concentration values. The same spiked samples were then measured by Cold Vapour Atomic Fluorescence Spectrometry (CV-AFS; a conventional method for detecting Hg^{2+}), and the results compared (Table 1). The concentrations of spiked samples are in good agreement, which indicates that the method can be applied to analyse Hg^{2+} in environmental water samples.

4. Conclusions

We have reported a facile, highly selective, and sensitive two-step sensing method based on an Hg^{2+}-regulated MSO molecular configuration switch and Hg^{2+}-modulated FRET with the aid of Ag^{+} as sensor activator. The configuration switching of cytosine and thymine bases in the presence of Ag^{+} and Hg^{2+} was demonstrated by NMR spectroscopy. The limit of detection of the proposed Hg^{2+} sensor is 100 pM, which is more than one order of magnitude lower than that reported when using DNAzymes and other reported "turn-off" MSO-based Hg^{2+} sensors. The limit of detection of the sensor is also two-orders of magnitude lower than the Hg^{2+} safe limit of 10 nM reported by the WHO and USEPA, with a broad detection range from 100 pM to 0.1 mM. The simplicity and feasibility of the assay was demonstrated by detecting Hg^{2+} in spiked water samples. The results described herein are a proof of concept, demonstrating that the method is suitable for monitoring applications with high sensitivity and specificity under the influence of environmentally relevant metal ions. The stability of the sensor can be further improved for its potential development as a cost-effective and useful tool for environmental monitoring.

Funding sources

This work was carried out initially with the financial support by the Universidad Nacional de Barranca, Peru [grant number RG92973], and completed with the help of the Universidad Nacional de Cañete, Peru [grant number RG99980].

CRediT authorship contribution statement

Noorhayati Idros: Conceptualization, Methodology, Investigation, Writing – original draft, Writing – review & editing, Visualization. **Katherine Stott:** Validation, Writing – review & editing, Visualization. **Jasmina Allen:** Validation. **Varun S. Kamboj:** Writing – review & editing. **Warren T. Corns:** Resources. **Hernán Verde-Luján:** Resources. **Luis De Los Santos Valladares:** Project administration. **Carlos Villanueva:** Funding acquisition. **Jorge H. Jhoncon:** Funding acquisition. **Daping Chu:** Resources. **Crispin.H.W. Barnes:** Resources, Project administration, Supervision.

Declaration of competing interest

The authors declare that they have no known competing financial interests or personal relationships that could have appeared to influence the work reported in this paper.

Acknowledgement

N. Idros and C. H. W. Barnes would like to thank Inés Garate and Luis Enrique Carrillo Díaz (from grant number RG92973), for their encouragement and constant support during the project. We must also thank Eustace P. G. Barnes, D. H. N. Perera and Peter J. Newton for helpful discussions on the field applications for the developed sensor in water analysis.

References

[1] L. Shi, Y. Li, Z. Liu, T. James, Y. Long, Simultaneous determination of Hg(II) and Zn (II) using a GFP inspired chromophore, Talanta 100 (2012) 401–404, https://doi.org/10.1016/j.talanta.2012.07.097.
[2] Y. Tian, Y. Wang, Y. Xu, Y. Liu, D. Li, C. Fan, A highly sensitive chemiluminescence sensor for detecting mercury (II) ions: a combination of Exonuclease III-aided signal amplification and graphene oxide-assisted background reduction, Sci. China Chem. 58 (3) (2015) 514–518, https://doi.org/10.1007/s11426-014-5258-9.
[3] M. Yuan, Y. Zhu, X. Lou, C. Chen, G. Wei, M. Lan, J. Zhao, Sensitive label-free oligonucleotide-based microfluidic detection of mercury (II) ion by using exonuclease I, Biosens. Bioelectron. 31 (1) (2012) 330–336, https://doi.org/10.1016/j.bios.2011.10.043.
[4] M. Zaib, M.M. Athar, A. Saeed, U. Farooq, Electrochemical determination of inorganic mercury and arsenic–A review, Biosens. Bioelectron. 74 (2015) 895–908, https://doi.org/10.1016/j.bios.2015.07.058.
[5] Z. Li, Y. Ni, S. Kokot, A new fluorescent nitrogen-doped carbon dot system modified by the fluorophore-labeled ssDNA for the analysis of 6-mercaptopurine and Hg (II), Biosens. Bioelectron. 74 (2015) 91–97, https://doi.org/10.1016/j.bios.2015.06.014.
[6] A.C. Bosch, B. O'Neill, G.O. Sigge, S.E. Kerwath, L.C. Hoffman, Mercury accumulation in Yellowfin tuna (Thunnus albacares) with regards to muscle type, muscle position and fish size, Food Chem. 190 (2016) 351–356, https://doi.org/10.1016/j.foodchem.2015.05.109.
[7] M. Xu, Z. Gao, Q. Wei, G. Chen, D. Tang, Label-free hairpin DNA-scaffolded silver nanoclusters for fluorescent detection of Hg^{2+} using exonuclease III-assisted target recycling amplification, Biosens. Bioelectron. 79 (2016) 411–415, https://doi.org/10.1016/j.bios.2015.12.081.
[8] J. Miller, J. Rowland, P. Lechler, M. Desilets, L. Hsu, Dispersal of mercury-contaminated sediments by geomorphic processes, sixmile canyon, Nevada, USA: implications to site characterization and remediation of fluvial environments, Water, Air, And Soil Pollution 86 (1–4) (1996) 373–388, https://doi.org/10.1007/bf00279168.
[9] J.S. Lee, M.S. Han, C.A. Mirkin, Colorimetric detection of mercuric ion (Hg^{2+}) in aqueous media using DNA-functionalized gold nanoparticles, Angew. Chem. 46 (22) (2007) 4093–4096, https://doi.org/10.1002/anie.200700269.
[10] X. Zuo, H. Zhang, Q. Zhu, W. Wang, J. Feng, X. Chen, A dual-color fluorescent biosensing platform based on WS2 nanosheet for detection of Hg(2+) and Ag(.), Biosens. Bioelectron. 85 (2016) 464–470, https://doi.org/10.1016/j.bios.2016.05.044.
[11] Epa gov, Retrieved, https://www.epa.gov/ground-water-and-drinking-water/national-primary-drinking-water-regulations#one, 2021. (Accessed 26 November 2021).
[12] S. Jia, C. Bian, J. Sun, J. Tong, S. Xia, A wavelength-modulated localized surface plasmon resonance (LSPR) optical fiber sensor for sensitive detection of mercury (II) ion by gold nanoparticles-DNA conjugates, Biosens. Bioelectron. 114 (2018) 15–21, https://doi.org/10.1016/j.bios.2018.05.004.
[13] L.P. Yu, X.P. Yan, Flow injection on-line sorption preconcentration coupled with cold vapor atomic fluorescence spectrometry and on-line oxidative elution for the determination of trace mercury in water samples, Atom. Spectros 25 (3) (2004) 145–153, https://doi.org/10.46770/AS.2004.03.006.
[14] S. Gil, I. Lavilla, C. Bendicho, Ultrasound-promoted cold vapor generation in the presence of formic acid for determination of mercury by atomic absorption spectrometry, Anal. Chem. 78 (17) (2006) 6260–6264, https://doi.org/10.1021/ac0606498.
[15] W. McShane, R. Pappas, V. Wilson-McElprang, D. Paschal, A rugged and transferable method for determining blood cadmium, mercury, and lead with inductively coupled plasma-mass spectrometry, Spectrochim. Acta B Atom Spectrosc. 63 (6) (2008) 638–644, https://doi.org/10.1016/j.sab.2008.03.016.
[16] B. Fong, T. Siu, J. Lee, S. Tam, Determination of mercury in whole blood and urine by inductively coupled plasma mass spectrometry, J. Anal. Toxicol. 31 (5) (2007) 281–287, https://doi.org/10.1093/jat/31.5.281.
[17] D. Malinovsky, R. Sturgeon, L. Yang, Anion-exchange chromatographic separation of Hg for isotope ratio measurements by multicollector ICPMS, Anal. Chem. 80 (7) (2008) 2548–2555, https://doi.org/10.1021/ac702190d.

[18] Y.K. Li, Y.R. Xu, Y. Huang, Y. Dai, Q.F. Hu, G.Y. Yang, Cold vapour generation and atomic fluorescence spectrometry for the determination of mercury, Asian J. Chem. 21 (4) (2009) 2893–2897.

[19] N. Bloom, W. Fitzgerald, Determination of volatile mercury species at the picogram level by low-temperature gas chromatography with cold-vapour atomic fluorescence detection, Anal. Chim. Acta 208 (1988) 151–161, https://doi.org/10.1016/s0003-2670(00)80743-6.

[20] N. Ferrua, S. Cerutti, J.A. Salonia, R.A. Olsina, L.D. Martinez, On-line preconcentration and determination of mercury in biological and environmental samples by cold vapor-atomic absorption spectrometry, J. Hazard Mater. 141 (3) (2007) 693–699, https://doi.org/10.1016/j.jhazmat.2006.07.028.

[21] X. Guo, X. Qian, L. Jia, A highly selective and sensitive fluorescent chemosensor for Hg^{2+}in neutral buffer aqueous solution, J. Am. Chem. Soc. 126 (8) (2004) 2272–2273, https://doi.org/10.1021/ja037604y.

[22] A. Caballero, R. Martínez, V. Lloveras, I. Ratera, J. Vidal-Gancedo, K. Wurst, A. Tárraga, P. Molina, J. Veciana, Highly selective chromogenic and redox or fluorescent sensors of Hg^{2+}in aqueous environment based on 1,4-disubstituted azines, J. Am. Chem. Soc. 127 (45) (2005) 15666–15667, https://doi.org/10.1021/ja0545766.

[23] E. Coronado, J.R. Galán-Mascarós, C. Martí-Gastaldo, E. Palomares, J.R. Durrant, R. Vilar, M. Gratzel, M.K. Nazeeruddin, Reversible colorimetric probes for mercury sensing, J. Am. Chem. Soc. 127 (35) (2005) 12351–12356, https://doi.org/10.1021/ja0517724.

[24] M.K. Nazeeruddin, D. Di Censo, R. Humphry-Baker, M. Grätzel, Highly selective and reversible optical, colorimetric, and electrochemical detection of mercury(II) by amphiphilic ruthenium complexes anchored onto mesoporous oxide films, Adv. Funct. Mater. 16 (2) (2006) 189–194, https://doi.org/10.1002/adfm.200500309.

[25] E. Palomares, R. Vilar, J.R. Durrant, Heterogeneous colorimetric sensor for mercuric saltsElectronic supplementary information (ESI) available: materials and methods, Chem. Commun. (4) (2004) 362, https://doi.org/10.1039/b314138a. See, http://www.rsc.org/suppdata/cc/b3/b314138a/.

[26] P. Chen, C. He, A general strategy to convert the MerR family proteins into highly sensitive and selective fluorescent biosensors for metal ions, J. Am. Chem. Soc. 126 (3) (2004) 728–729, https://doi.org/10.1021/ja0383975.

[27] H. Kim, D. Park, M. Hyun, Y. Shim, Determination of HgII ion with a 1,11-Bis(8-quinoyloxy)-3,6,9-trioxaundecane-Modified glassy carbon electrode using spin-coating technique, Electroanalysis 10 (5) (1998) 303–306, https://doi.org/10.1002/(sici)1521-4109(199804)10:5<303::aid-elan303>3.0.co;2-a.

[28] M.A. Nolan, S.P. Kounaves, Microfabricated array of iridium microdisks as a substrate for direct determination of Cu2+or Hg2+Using square-wave anodic stripping voltammetry, Anal. Chem. 71 (16) (1999) 3567–3573, https://doi.org/10.1021/ac990126i.

[29] Y. Zhao, Z. Zhong, Tuning the sensitivity of a foldamer-based mercury sensor by its folding energy, J. Am. Chem. Soc. 128 (31) (2006) 9988–9989, https://doi.org/10.1021/ja062001i.

[30] K. Srinivasan, K. Subramanian, K. Murugan, G. Benelli, K. Dinakaran, Fluorescence quenching of MoS2 nanosheets/DNA/silicon dot nanoassembly: effective and rapid detection of Hg2+ ions in aqueous solution, Environ. Sci. Pollut. Control Ser. 25 (11) (2018) 10567–10576, https://doi.org/10.1007/s11356-018-1472-x.

[31] Y. Wang, L. Wang, F. An, H. Xu, Z. Yin, S. Tang, H. Yang, H. Song, Graphitic carbon nitride supported platinum nanocomposites for rapid and sensitive colorimetric detection of mercury ions, Anal. Chim. Acta 980 (2017) 72–78, https://doi.org/10.1016/j.aca.2017.05.019.

[32] S. Babkina, N. Ulakhovich, Complexing of heavy metals with DNA and new bioaffinity method of their determination based on amperometric DNA-based biosensor, Anal. Chem. 77 (17) (2005) 5678–5685, https://doi.org/10.1021/ac050727b.

[33] A. Ono, H. Togashi, Highly selective oligonucleotide-based sensor for mercury(II) in aqueous solutions, Angew. Chem. Int. Ed. 43 (33) (2004) 4300–4302, https://doi.org/10.1002/anie.200454172.

[34] Y. Tanaka, S. Oda, H. Yamaguchi, Y. Kondo, C. Kojima, A. Ono, 15N−15NJ-Coupling across HgII: direct observation of HgII-mediated T−T base pairs in a DNA duplex, J. Am. Chem. Soc. 129 (2) (2007) 244–245, https://doi.org/10.1021/ja065552h.

[35] Y. Miyake, H. Togashi, M. Tashiro, H. Yamaguchi, S. Oda, M. Kudo, Y. Tanaka, Y. Kondo, R. Sawa, T. Fujimoto, T. Machinami, A. Ono, MercuryII-mediated formation of Thymine−HgII−Thymine base pairs in DNA duplexes, J. Am. Chem. Soc. 128 (7) (2006) 2172–2173, https://doi.org/10.1021/ja056354d.

[36] T. Li, S. Dong, E. Wang, Label-free colorimetric detection of aqueous mercury ion (Hg^{2+}) using Hg^{2+}-modulated G-quadruplex-based DNAzymes, Anal. Chem. 81 (6) (2009) 2144–2149, https://doi.org/10.1021/ac900188y.

[37] T. Li, B. Li, E. Wang, S. Dong, G-quadruplex-based DNAzyme for sensitive mercury detection with the naked eye, Chem. Commun. (24) (2009) 3551, https://doi.org/10.1039/b903993g.

[38] X. Xue, F. Wang, X. Liu, One-step, room temperature, colorimetric detection of mercury (Hg^{2+}) using DNA/nanoparticle conjugates, J. Am. Chem. Soc. 130 (11) (2008) 3244–3245, https://doi.org/10.1021/ja076716c.

[39] X. Zuo, H. Wu, J. Toh, S. Li, Mechanism of mercury detection based on interaction of single-strand DNA and hybridized DNA with gold nanoparticles, Talanta 82 (5) (2010) 1642–1646, https://doi.org/10.1016/j.talanta.2010.07.031.

[40] G. Chen, W. Chen, Y. Yen, C. Wang, H. Chang, C. Chen, Detection of mercury(II) ions using colorimetric gold nanoparticles on paper-based analytical devices, Anal. Chem. 86 (14) (2014) 6843–6849, https://doi.org/10.1021/ac5008688.

[41] N. Kanayama, T. Takarada, M. Maeda, Rapid naked-eye detection of mercury ions based on non-crosslinking aggregation of double-stranded DNA-carrying gold nanoparticles, Chem. Commun. 47 (7) (2011) 2077–2079, https://doi.org/10.1039/c0cc05171c.

[42] F. Xuan, X. Luo, I. Hsing, Conformation-dependent exonuclease III activity mediated by metal ions reshuffling on thymine-rich DNA duplexes for an ultrasensitive electrochemical method for Hg^{2+} detection, Anal. Chem. 85 (9) (2013) 4586–4593, https://doi.org/10.1021/ac400228q.

[43] E. Xiong, L. Wu, J. Zhou, P. Yu, X. Zhang, J. Chen, A ratiometric electrochemical biosensor for sensitive detection of Hg 2+ based on thymine–Hg 2+ –thymine structure, Anal. Chim. Acta 853 (2015) 242–248, https://doi.org/10.1016/j.aca.2014.10.015.

[44] F. Yang, X. Zuo, Z. Li, W. Deng, J. Shi, G. Zhang, Q. Huang, S. Song, C. Fan, A bubble-mediated intelligent microscale electrochemical device for single-step quantitative bioassays, Adv. Mater. 26 (27) (2014) 4671–4676, https://doi.org/10.1002/adma.201400451.

[45] M. Liu, Z. Wang, S. Zong, H. Chen, D. Zhu, L. Wu, G. Hu, Y. Cui, SERS detection and removal of mercury(II)/Silver(I) using oligonucleotide-functionalized core/shell magnetic silica sphere@Au nanoparticles, ACS Appl. Mater. Interfaces 6 (10) (2014) 7371–7379, https://doi.org/10.1021/am5006282.

[46] E. Chung, R. Gao, J. Ko, N. Choi, D.W. Lim, E.K. Lee, S. Chang, J. Choo, Trace analysis of mercury(ii) ions using aptamer-modified Au/Ag core–shell nanoparticles and SERS spectroscopy in a microdroplet channel, Lab Chip 13 (2) (2013) 260–266, https://doi.org/10.1039/c2lc41079f.

[47] L. Xu, H. Yin, W. Ma, H. Kuang, L. Wang, C. Xu, Ultrasensitive SERS detection of mercury based on the assembled gold nanochains, Biosens. Bioelectron. 67 (2015) 472–476, https://doi.org/10.1016/j.bios.2014.08.088.

[48] X. Ding, L. Kong, J. Wang, F. Fang, D. Li, J. Liu, Highly sensitive SERS detection of Hg^{2+} ions in aqueous media using gold nanoparticles/graphene heterojunctions, ACS Appl. Mater. Interfaces 5 (15) (2013) 7072–7078, https://doi.org/10.1021/am401373e.

[49] Y. Zeng, L. Wang, L. Zeng, A. Shen, J. Hu, A label-free SERS probe for highly sensitive detection of Hg2+ based on functionalized Au@Ag nanoparticles, Talanta 162 (2017) 374–379, https://doi.org/10.1016/j.talanta.2016.09.062.

[50] Y. Zeng, J. Ren, A. Shen, J. Hu, Field and pretreatment-free detection of heavy-metal ions in organic polluted water through an alkyne-coded SERS test kit, ACS Appl. Mater. Interfaces 8 (41) (2016) 27772–27778, https://doi.org/10.1021/acsami.6b09722.

[51] X. Ding, L. Kong, J. Wang, F. Fang, D. Li, J. Liu, Highly sensitive SERS detection of Hg^{2+} ions in aqueous media using gold nanoparticles/graphene heterojunctions, ACS Appl. Mater. Interfaces 5 (15) (2013) 7072–7078, https://doi.org/10.1021/am401373e.

[52] K. Chen, G. Lu, J. Chang, S. Mao, K. Yu, S. Cui, J. Chen, Hg(II) ion detection using thermally reduced graphene oxide decorated with functionalized gold nanoparticles, Anal. Chem. 84 (9) (2012) 4057–4062, https://doi.org/10.1021/ac3000336.

[53] T. Zhang, Z. Cheng, Y. Wang, Z. Li, C. Wang, Y. Li, Y. Fang, Self-Assembled 1-octadecanethiol monolayers on graphene for mercury detection, Nano Lett. 10 (11) (2010) 4738–4741, https://doi.org/10.1021/nl1032556.

[54] A. Sadrolhosseini, A. Noor, A. Bahrami, H. Lim, Z. Talib, M. Mahdi, Application of polypyrrole multi-walled carbon nanotube composite layer for detection of mercury, lead and iron ions using surface plasmon resonance technique, PLoS One 9 (4) (2014), e93962, https://doi.org/10.1371/journal.pone.0093962.

[55] T. Liu, J.X. Dong, S.G. Liu, N. Li, S.M. Lin, Y.Z. Fan, L.J. Lei, H.Q. Luo, N.B. Li, Carbon quantum dots prepared with polyethyleneimine as both reducing agent and stabilizer for synthesis of Ag/CQDs composite for Hg^{2+} ions detection, J. Hazard Mater. 322 (2017) 430–436, https://doi.org/10.1016/j.jhazmat.2016.10.034.

[56] M. Zareh Jonaghani, H. Zali-Boeini, Highly selective fluorescent and colorimetric chemosensor for detection of Hg 2+ ion in aqueous media, Spectrochim. Acta Mol. Biomol. Spectrosc. 178 (2017) 66–70, https://doi.org/10.1016/j.saa.2017.01.065.

[57] T. Yu, T. Zhang, W. Zhao, J. Xu, H. Chen, A colorimetric/fluorescent dual-mode sensor for ultra-sensitive detection of Hg^{2+}, Talanta 165 (2017) 570–576, https://doi.org/10.1016/j.talanta.2017.01.026.

[58] L. Tan, Z. Chen, C. Zhang, X. Wei, T. Lou, Y. Zhao, Colorimetric detection of Hg2+ Based on the growth of aptamer-coated AuNPs: the effect of prolonging aptamer strands, Small 13 (14) (2017) 1603370, https://doi.org/10.1002/smll.201603370.

[59] D. Tan, Y. He, X. Xing, Y. Zhao, H. Tang, D. Pang, Aptamer functionalized gold nanoparticles based fluorescent probe for the detection of mercury (II) ion in aqueous solution, Talanta 113 (2013) 26–30, https://doi.org/10.1016/j.talanta.2013.03.055.

[60] Y. Zhou, Z. Xu, J. Yoon, Fluorescent and colorimetric chemosensors for detection of nucleotides, FAD and NADH: highlighted research during 2004–2010, Chem. Soc. Rev. 40 (5) (2011) 2222–2235, https://doi.org/10.1039/c0cs00169d.

[61] D. Quang, J. Kim, Fluoro- and chromogenic chemodosimeters for heavy metal ion detection in solution and biospecimens, Chem. Rev. 110 (10) (2010) 6280–6301, https://doi.org/10.1021/cr100154p.

[62] X. Chen, Y. Zhou, X. Peng, J. Yoon, Fluorescent and colorimetric probes for detection of thiols, Chem. Soc. Rev. 39 (6) (2010) 2120–2135, https://doi.org/10.1039/b925092a.

[63] J.F. Zhang, Y. Zhou, J. Yoon, J. Kim, Recent progress in fluorescent and colorimetric chemosensors for detection of precious metal ions (silver, gold and platinum ions), Chem. Soc. Rev. 40 (7) (2011) 3416, https://doi.org/10.1039/c1cs15028f.

[64] S. Su, J.W. Fan, B. Xue, L.H. Yuwen, X.F. Liu, D. Pan, C.H. Fan, L.H. Wang, DNA-conjugated quantum dot nanoprobe for high-sensitivity fluorescent detection of DNA and micro-RNA, ACS Appl. Mater. Interfaces 6 (2) (2014) 1152–1157, https://doi.org/10.1021/am404811j.

[65] H. Xu, S. Gao, Q. Yang, D. Pan, L. Wang, C. Fan, Amplified fluorescent recognition of G-quadruplex folding with a cationic conjugated polymer and DNA intercalator, ACS Appl. Mater. Interfaces 2 (11) (2010) 3211–3216, https://doi.org/10.1021/am1006854.
[66] D. Li, S. Song, C. Fan, Target-responsive structural switching for nucleic acid-based sensors, Acc. Chem. Res. 43 (5) (2010) 631–641, https://doi.org/10.1021/ar900245u.
[67] C. Liu, C. Huang, H. Chang, Highly selective DNA-based sensor for lead(II) and mercury(II) ions, Anal. Chem. 81 (6) (2009) 2383–2387, https://doi.org/10.1021/ac8022185.
[68] X. He, Z. Qing, K. Wang, Z. Zou, H. Shi, J. Huang, Engineering a unimolecular multifunctional DNA probe for analysis of Hg^{2+} and Ag^{+}, Anal. Methods 4 (2) (2012) 345, https://doi.org/10.1039/c2ay05823e.
[69] T. Uchiyama, T. Miura, H. Takeuchi, T. Dairaku, T. Komuro, T. Kawamura, et al., Raman spectroscopic detection of the T-Hg II -T base pair and the ionic characteristics of mercury, Nucleic Acids Res. 40 (12) (2012) 5766–5774, https://doi.org/10.1093/nar/gks208.
[70] L. Guo, N. Yin, G. Chen, Photoinduced electron transfer mediated by π-stacked Thymine−Hg^{2+}−Thymine base pairs, J. Phys. Chem. C 115 (11) (2011) 4837–4842, https://doi.org/10.1021/jp1083482.
[71] J. Zhang, S. Song, L. Wang, D. Pan, C. Fan, A gold nanoparticle-based chronocoulometric DNA sensor for amplified detection of DNA, Nat. Protoc. 2 (11) (2007) 2888–2895, https://doi.org/10.1038/nprot.2007.419.
[72] G. Wang, Y. Lu, C. Yan, Y. Lu, DNA-functionalization gold nanoparticles based fluorescence sensor for sensitive detection of Hg2+ in aqueous solution, Sensor. Actuator. B Chem. 211 (2015) 1–6, https://doi.org/10.1016/j.snb.2015.01.051.
[73] Z. Chen, L. Li, X. Mu, H. Zhao, L. Guo, Electrochemical aptasensor for detection of copper based on a reagentless signal-on architecture and amplification by gold nanoparticles, Talanta 85 (1) (2011) 730–735, https://doi.org/10.1016/j.talanta.2011.04.056.
[74] C. Schneider, W. Rasband, K. Eliceiri, NIH Image to ImageJ: 25 years of image analysis, Nat. Methods 9 (7) (2012) 671–675, https://doi.org/10.1038/nmeth.2089.
[75] D. Gruenwedel, NUCLEIC ACIDS | Properties and Determination, Encyclopedia Of Food Sciences and Nutrition, 2003, pp. 4147–4152, https://doi.org/10.1016/b0-12-227055-x/00836-1.
[76] R.R. Alexander, J.M. Griffiths, Basic Biochemical Methods, second ed., Wiley, 1993.
[77] A. Ono, S. Cao, H. Togashi, M. Tashiro, T. Fujimoto, T. Machinami, et al., Specific interactions between silver(i) ions and cytosine–cytosine pairs in DNA duplexes, Chem. Commun. (39) (2008) 4825, https://doi.org/10.1039/b808686a.
[78] P. Huang, J. Liu, Sensing parts-per-trillion Cd^{2+}, Hg^{2+}, and Pb^{2+} collectively and individually using phosphorothioate DNAzymes, Anal. Chem. 86 (12) (2014) 5999–6005, https://doi.org/10.1021/ac501070a.
[79] P. Huang, F. Wang, J. Liu, Cleavable molecular beacon for Hg^{2+} detection based on phosphorothioate RNA modifications, Anal. Chem. 87 (13) (2015) 6890–6895, https://doi.org/10.1021/acs.analchem.5b01362.
[80] J. Chen, J. Pan, S. Chen, A naked-eye colorimetric sensor for Hg^{2+} monitoring with cascade signal amplification based on target-induced conjunction of split DNAzyme fragments, Chem. Commun. 53 (73) (2017) 10224–10227, https://doi.org/10.1039/c7cc05445a.
[81] C. Liu, C. Huang, H. Chang, Highly selective DNA-based sensor for lead(II) and mercury(II) ions, Anal. Chem. 81 (6) (2009) 2383–2387, https://doi.org/10.1021/ac8022185.
[82] X. He, Z. Qing, K. Wang, Z. Zou, H. Shi, J. Huang, Engineering a unimolecular multifunctional DNA probe for analysis of Hg^{2+} and Ag^{+}, Anal. Methods 4 (2) (2012) 345, https://doi.org/10.1039/c2ay05823e.